The isobutylene was removed by freeze–pump–thaw degassing before the polymerization was started (see the Experimental Section).
(15) The second block contained a small amount of polybenzonorbornadiene due to residual monomer present from the previous block. Typically the blocks synthesized contained a minor amount of the other polymer. The living polymer decomposes in the absence of monomer at 70 °C. Therefore, the polymerizations were run to 95% completion.
(16) The procedure for the synthesis of "titanocene" was provided by the J. E. Bercaw research group, California Institute of Technology.
(17) The significant quantities of ozone present in the atmosphere in Pasadena, CA, may have accelerated this process. Samples of polynorbornene containing 1% BHT (2,6-di-*tert*-butyl-4-methylphenol) by weight were completely air-stable over several months.
(18) Gilliom, L. R. Ph.D. Thesis, California Institute of Technology.
(19) Thermal instability of metallacycles in solution has been previously observed. See ref 6.
(20) Yau, W. W.; Kirkland, J. J.; Bly, D. D. *Modern Size-Exclusion Chromatography*; Wiley: New York, 1979.
(21) (a) Wittig, G.; Knauss, T. *Chem. Ber.* **1958**, *91*, 895. (b) Eisch, J. J.; Burlinson, N. E. *J. Am. Chem. Soc.* **1976**, *98*, 753.
(22) (a) Alder, K.; Stein, G. *Annu.* **1933**, *504*, 219. (b) Bartlett, P. D.; Goldstein, I. S. *J. Am. Chem. Soc.* **1947**, *69*, 2553.

# Synthesis and Properties of Segmented and Block Poly(hydroxy ether–siloxane) Copolymers

**J. L. Hedrick,* B. Haidar, T. P. Russell, and D. C. Hofer**

*IBM Research, Almaden Research Center, 650 Harry Road, San Jose, California 95120-6099.* *Received January 14, 1988*

ABSTRACT: Segmented or block poly(hydroxy ether–siloxane) copolymers that are both chemically cross-linked and microphase separated have been synthesized. In this work, the molecular weight of the siloxane block lengths varied from 900 to 12 400 g/mol, and the hydroxy ether block lengths varied from 340 to 3700 g/mol. Calorimetric, dynamic mechanical, and small-angle X-ray scattering measurements showed that higher block length oligomers gave networks with a more well-defined two-phase morphology. The mechanical behavior of the networks depended on the continuous phase with ultimate elongations ranging from 50 to 180% and moduli ranging from 1.0 to 600 MPa.

## Introduction

Organosiloxane-based elastomers have many desirable properties including low-temperature flexibility, thermal and oxidative stability, low surface energy, high compressibility, and high gas permeability. Consequently, these elastomers have been used widely. These materials have a low glass transition temperature, $T_g$, (ca. −123 °C), and at room temperature, the molecular segments are sufficiently mobile such that cracks readily initiate and propagate.[1] The low melting point (−40 °C), however, prevents strain-induced crystallization,[2-4] which leads to reduced toughness.

Particulate fillers are commonly used to increase the toughness. Reinforcement may also be achieved by preparing model networks containing both long and short chains.[5-7] These bimodal networks showed enhanced tensile strength as the fraction of short chains is increased. Haidar and Smith[8] have shown that the tensile strength and relaxation rate pass through a maximum between 30 and 40% by weight short chains. The increased relaxation rate results from decreased chain mobility. Thus, reinforcement may also be achieved by increasing the viscoelastic response of the network.

The synthesis of multiphase systems in the form of block, graft, or segmented copolymers is a viable alternative in the design of elastomeric materials with good mechanical properties.[9-11] Generally, these materials are composed of hard and soft segments or blocks. The morphology of these elastomers will depend on the relative molecular weights of the individual blocks, whereas the segmental interactions will control the phase purity. Smith[12-14] has investigated the mechanical properties of several segmented and block copolymers. The hard segment domains in these elastomeric systems were found to impede the formation of and slow the growth of microcracks as well as prevent cracks from attaining a critical size where they become unstable. Furthermore, the incorporation of a second phase serves to increase the internal viscosity, distributing the stress more uniformly throughout the specimen, thereby reducing stress concentrations.

Segmented or block copolymers containing a sufficient concentration of a hard component whose $T_g$ is well above the test temperature are more effective in imparting strength than particulate fillers since the domains are dispersed uniformly and can undergo deformation. Block copolymers of siloxane with poly(arylene ether sulfones),[15,16] poly(arylene esters),[17,18] polycarbonates,[19-21] and other hard segments[9] are classic examples of single-component, microphase-separated polymers. These are typically prepared by the condensation of silylamine-terminated siloxane oligomers with phenolic hydroxyl-terminated hard blocks affording a perfectly alternating $(A–B)_n$ structure. Microphase separation is found provided sufficiently long block lengths are used and the mechanical response is dominated by the continuous phase.[16,22] McGrath and co-workers[25,26] have recently reported a series of segmented copolymers prepared by an oligomer–monomer synthetic approach. The linkage between the blocks is formed simultaneously with the growth of the second block, where the nature of the linkage depends upon the functional end groups of the preformed oligomer and monomer. This synthetic route is similar to the preparation of Hytrel polyurethane and Estane urea-linked copolymers. A series of novel siloxane–imide, siloxane–hydroxy ether,[24] and siloxane–urea[23,26] copolymers were prepared, where apparent strong intermolecualr interactions within the hard segment provided microphase-sep-

0024-9297/88/2221-1967$01.50/0 

arated morphologies and good mechanical properties.[26]

In this paper, we extend earlier investigations on the poly(hydroxy ether–siloxane) copolymers reported by McGrath et al.[26] and Hedrick et al.[27,28] A detailed synthetic procedure and a basic structure–property relation for both the segmented and block copolymer systems is presented.

## Experimental Section

Octamethylcyclotetrasiloxane ($D_4$) and 1,3-bis(aminopropyl)-tetramethyldisiloxane were purchased from Petrarch. The tetramethylammonium hydroxide pentahydrate (Aldrich) was used without further purification. DER 332 (diglycidyl ether of bisphenol A (DGEBA)), referred to as epoxy 1, and DER 667, denoted epoxy 4, were supplied from Dow Chemical Co. and have number-average molecular weights of 340 and 3700 g/mol, respectively. Epon resins 1001F (epoxy 2) and 1004 (epoxy 3) were obtained from Shell Chemical Co. and have number-average molecular weights of 1150 and 1800, respectively.

The $\alpha,\omega$-bis(aminopropyl)-poly(dimethylsiloxane) oligomers of various molecular weights were synthesized by base (tetramethylammonium hydroxide pentahydrate) catalyzed bulk anionic equilibrium reaction of $D_4$ with 1,3-bis(aminopropyl)tetramethyldisiloxane end blocker. The equilibration was maintained at 80 °C for 24 h, and then the reaction temperature was increased to 150 °C to decompose the catalyst. The oligomers were vacuum distilled at 150 °C to remove the equilibrium cyclics.

The aminopropyl-terminated poly(dimethylsiloxane) oligomers and the DGEBA or the epoxy-terminated hydroxy ether oligomers were allowed to react at 50 °C for 36 h in chloroform or for those copolymers containing the higher molecular weight hydroxy ether oligomers in a 50/50 mixture of chloroform/tetrahydrofuran (~35 wt % solids). The solutions were cast into films on cellophane, and the solvent or solvent mixture was allowed to evaporate slowly (24 h). The solid films were then cured at 100 °C (1 h) and post cured at 120° (1 h).

The number-average molecular weights of the aminopropyl-terminated siloxane oligomers were determined by titration with a Fisher computer-aided titrimeter. The siloxane oligomers were dissolved in isopropanol and titrated with 0.1 N HCl. The epoxy-terminated hydroxy ether oligomers were dissolved in a 2:1 mixture of chlorobenzene and acetic acid and titrated with 0.01 N HBr. Glass transition temperatures and kinetic measurements were performed on a Du Pont DSC 910 at a 10 °C/min heating rate. Swelling measurements were performed in chloroform (23 °C) for 72 h. Ammonia soak measurements were made in a sealed desiccator (23 °C) with a beaker of ammonium hydroxide submersed in chloroform for 48 h.

Stress–strain measurements were made on an Instron at a strain rate of 10 mm/min (22 °C). The dynamic mechanical measurements were performed on a Polymer Laboratories dynamic mechanical thermal analyzer (DMTA) at 10 Hz and a heating rate of 3 °C/min. Due to the sensitivity limit of the DMTA, these measurements were carried out in the bending mode at temperatures just below the $T_g$ of the hard segment (~30 °C) for those samples that did not crystallize, and, for the remaining samples, the bending mode was used up to the melting point of the siloxane component (~−40 °C). The shear mode was used above these temperatures.

Static small-angle X-ray scattering measurements were obtained with a Kratky slit-collimated camera with Ni-filtered Cu K$\alpha$ radiation. A standard focus, sealed X-ray tube operated at 40 kV and 20 mA served as the source. Scattered radiation, collected with a TEC-205 detector, was discriminated electronically prior to storage on a Tracor Northern 1705 multichannel analyzer. The scattering profiles were corrected for electronic noise, parasitic scattering, and detector homogeneity in the standard manner. All data were desmeared by using the methods of Vonk[29] and Glatter.[30,31]

Time-resolved scattering measurements were performed on Beamline I-4 at the Stanford Synchrotron Radiation Laboratory. X-rays emanating from the storage ring were focused vertically with a 50-cm platinum-coated quartz mirror bent asymmetrically to approximate an ellipse and tilted at 5 mrad to the incident beam. Horizontal focusing and monochromatization of the beam was accomplished with a bent Si (111) crystal oriented such that X-rays of wavelength 1.429 Å entered the experimental area. Monitors before and after the sample continuously recorded the change in the flux incident on the sample and transmitted beam. Scattered radiation was collected on a Reticon 1024S self-scanning photodiode array. The data were then processed with CAMAC electronics and stored on a hard disk for future use. At the specimen the beam was 1 mm × 400 μm, which could easily pass through the 2-mm hole in the Mettler FP85 hot stage used to heat the sample. More detailed descriptions of the facility can be found elsewhere.[32,33]

**Scheme I**

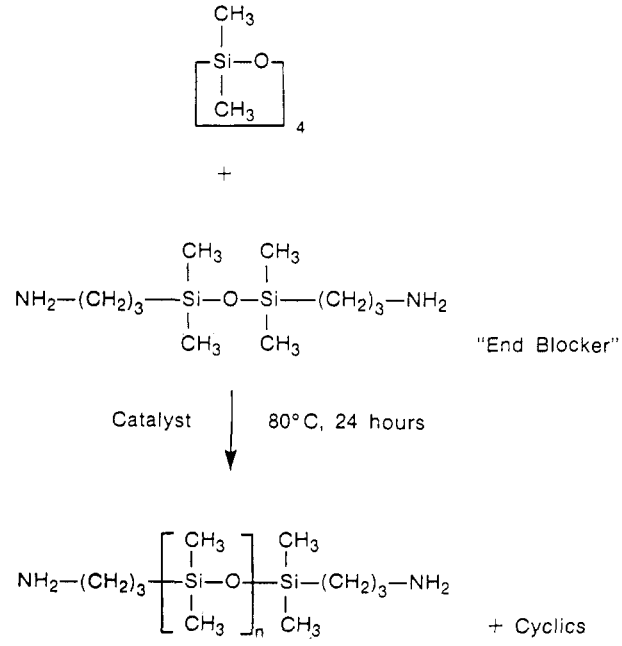


**Table I**
**Characteristics of Bis(aminopropyl)-Terminated Dimethylsiloxane Oligomers**

| no. | $\langle M_n \rangle$, g/mol | $T_g$,[a] °C | $T_c$, °C | $T_M$, °C |
|---|---|---|---|---|
| 1 | 900 | −114 | | |
| 2 | 1250 | −117 | | |
| 3 | 2600 | −120 | | |
| 4 | 3900 | −121 | −77 | −45, −39 |
| 5 | 5400 | −121 | −67 | −42 |
| 6 | 8500 | −121 | | |
| 7 | 12400 | −122 | −70 | −40, −36 |

[a] Differential scanning calorimetry (DSC), 10 °C/min heating rate.

## Results and Discussion

Aminopropyl-terminated poly(dimethylsiloxane) oligomers of various molecular weights were synthesized by a bulk anionic equilibration reaction with a basic catalyst as shown in Scheme I.[34] The bis(aminopropyl)tetramethyldisiloxane end-blocking agent was reacted with octamethylcyclotetrasiloxane ($D_4$) at 80 °C with tetramethylammonium hydroxide pentahydrate as the catalyst.[34,35] The ratio of the end blocker to $D_4$ controls the molecular weight of the oligomers. In the early stages of these bulk polymerizations the viscosities were high. Apparently, the cyclic tetramer of dimethylsiloxane is more reactive than the end blocker, and the ring opening of these cyclic tertamers affords high molecular weight. The chain transfer to the bis(aminopropyl)tetramethyldisiloxane decreased the viscosity according to the desired molecular weight. Upon completion of the polymerization (24 h), the reaction was heated to 150 °C to decompose the tetramethylammonium siloxanolate catalyst.[23,25,34] This de-

**Table II**
**Characteristics of Hydroxy Ether Oligomers and Diglycidyl Ether of Bisphenol A**

| sample | $\langle M_n \rangle$, g/mol | PI | thermal analysis,[a] °C $T_g$ | $T_m$ |
|---|---|---|---|---|
| epoxy 1 | 340 | | | 40 |
| epoxy 2 | 1150 | 2.0 | 47 | |
| epoxy 3 | 1800 | 2.3 | 57 | |
| epoxy 4 | 3700 | 2.5 | 76 | |

[a] DSC, 10 °C/min heating rate.

composition leads to volatiles including methanol and dimethylamine, which are easily removed at these temperatures. Table I contains the oligomers synthesized and their characterization. The number-average molecular weights, ranging from 900 to 12 500 g/mol, were determined by potentiometric titration of the end groups.[34,36] The high molecular weight oligomers showed $T_g$ values of ca. −120 °C and crystallized with a melting point of ca. −40 °C. In some instances a dual melting point was observed, which is consistent with earlier reports.[16] The low molecular weight oligomers have a slightly higher $T_g$ arising, most likely, from end groups.

In the preparation of siloxane-containing networks with a dispersed hard phase, the judicious choice of the co-block is crucial in obtaining both network formation and microphase separation. In our work, we have used poly(hydroxy ethers), which are engineering thermoplastics and exhibit tough ductile mechanical properties.[37-39] Several synthetic approaches have been employed for the preparation of high molecular weight poly(hydroxy ethers). A one-step approach reacting bisphenol with epichlorohydrin has been used to prepare a number of homopolymers and copolymers.[37,38] Alternatively, diglycidyl ether of bisphenol A may be reacted with the metal salt of bisphenol A on other bisphenols.[39] Each synthetic route proceeds via a more reactive bisphenate intermediate of the bisphenol and produces an alkoxide upon ring opening of the epoxide. The alkoxide formed is a stronger base than the bisphenate and may react with an epoxide, leading to branching. However, this branching has been reported to be minimal at lower molecular weights.[40,41] The molecular weight characteristics and the thermal transitions of the epoxy-terminated hydroxy ether oligomers and the diglycidyl ether of bisphenol A (DGEBA) are shown in Table II. Molecular weights ranging from 340 (monomer) to 3700 g/mol were determined by a potentiometric titration with HBr in glacial acetic acid.[24,28] The polydispersity index, PI ranges from 2.0 to 2.5 and increases with the number average molecular weight. The DGEBA has a crystalline melting point of 40 °C, and the oligomers have $T_g$ values ranging from 47 to 76 °C.

Several approaches were used in the preparation of segmented or block poly(hydroxy ether–siloxane) copolymers. The first synthetic route involves an oligomer–monomer route where the hydroxy ether linkage is formed simultaneously with the growth of the second block. The difunctional DGEBA was reacted with a stoichiometric amount of the tetrafunctional aminopropyl-terminated poly(dimethylsiloxane) oligomers to prepare poly(hydroxy ether–siloxane) copolymer networks as illustrated in Scheme II. The DGEBA was used as both a chain extender and cross-linker. This reaction is similar to the preparation of polyurethanes involving both monomers and preformed functional oligomers.

The second synthetic approach used employs preformed functionally terminated oligomers. Epoxy-terminated poly(hydroxy ether) oligomers were reacted with the

**Scheme II**

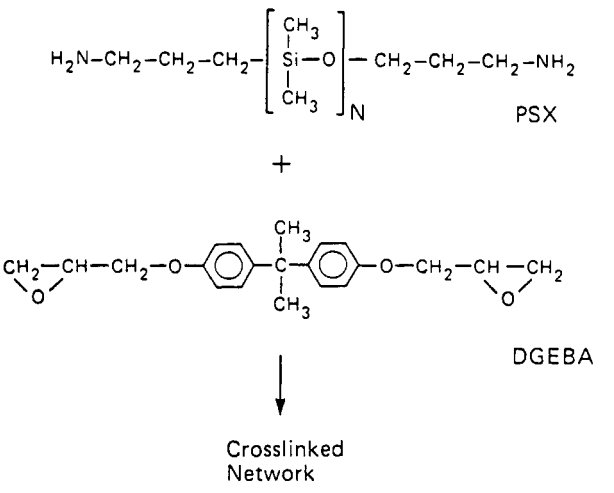


**Scheme III**

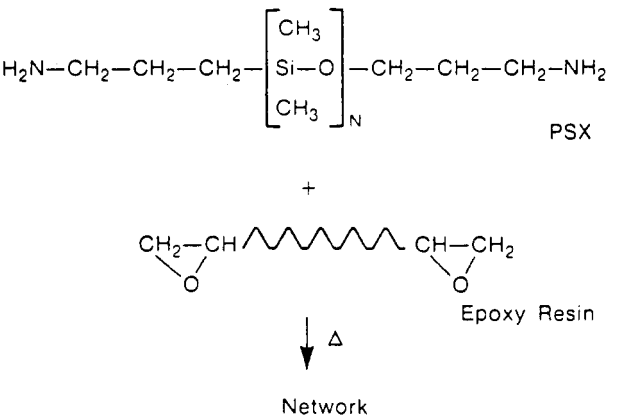


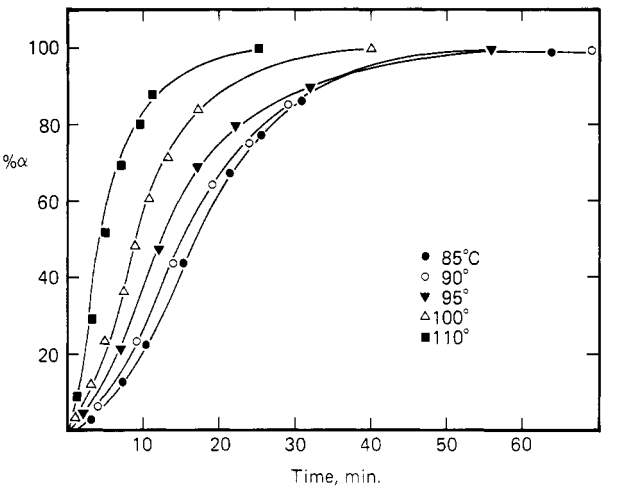


**Figure 1.** Percent conversion, $\alpha$, versus time for the reaction of DGEBA with an aminopropyl-terminated siloxane oligomer of 900 g/mol molecular weight of several temperatures.

aminopropyl-terminated poly(dimethylsiloxane) oligomers, producing a network structure as shown in Scheme III. In both synthetic routes, chloroform or for those reactions involving higher hydroxy ether block lengths a chloroform/tetrahydrofuran mixture was required in the early stages of the copolymerization to facilitate mixing and the initial polymerization of the two components. The solutions were cast and cured as described previously. Figure 1 contains the percent conversion, $\alpha$, as a function of time at several temperatures for the reaction of DGEBA with an aminopropyl-terminated siloxane oligomer of 900 g/mol

**Table III**
**Characteristics of Poly(hydroxy ether-siloxane) Networks[a]**

| no. | $\langle M_n \rangle$ (PSX) | wt % hard segment | thermal analysis,[b] °C | | | |
|---|---|---|---|---|---|---|
| | | | $T_g$ | $T_c$ | $T_m$ | $T_g$ |
| 1 | 900 | 50 | -110 | | | 27 |
| 2 | 1250 | 40 | -107 | | | 20 |
| 3 | 2600 | 23 | -110 | | | 18 |
| 4 | 3900 | 17 | -119 | | | 10 |
| 5 | 5400 | 13 | -119 | | | 10 |
| 6 | 8500 | 7 | -120 | -80 | -52 | 12 |
| 7 | 12400 | 6 | -120 | | -47 | |

[a] Less than 3 wt % extractables after cure. [b] DSC, 10 °C/min heating rate.

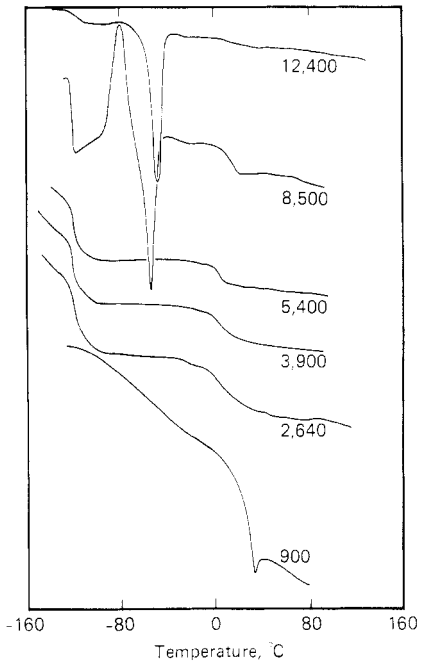


**Figure 2.** DSC thermograms for the poly(hydroxy ether–siloxane) networks synthesized via the monomer–oligomer approach with molecular weight of the siloxane blocks or segments ranging from 900 to 12 400 g/mol.

molecular weight. These results are consistent with those reported earlier[34] on similar systems. Clearly, a cure at 100 °C for 1 and a postcure at 120 °C for an additional hour is sufficient for full network formation. Perfectly alternating sequence distributions were obtained from the monomer or oligomers bearing mutually reactive end groups. The average molecular weight of the blocks, segments, or length between cross-length junctions are identical with the corresponding oligomer or monomer.

The characteristics of the poly(hydroxy ether–siloxane) networks synthesized via monomer–oligomer synthetic approach are given in Table III. The networks were characterized by both swelling measurements and thermal analyses. In each of the networks, less than 3% sol fraction was observed, indicating that full network formation was realized. Surprisingly, two glass transition temperatures were observed, showing that these materials were not only chemically cross-linked but microphase separated as well. Similar results were observed in another series of segmented siloxane–urea copolymers reported by Yilgor and McGrath[23] The glass transition temperature of the hard segment of the poly(hydroxy ether–siloxane) networks ranged from 10 to 27 °C, depending on the siloxane block length or the weight percent hard segment as shown in the DSC thermograms of Figure 2. The hard segment is believed to be composed of the monomer (DGEBA) unit and the contributions from the end groups of the siloxane

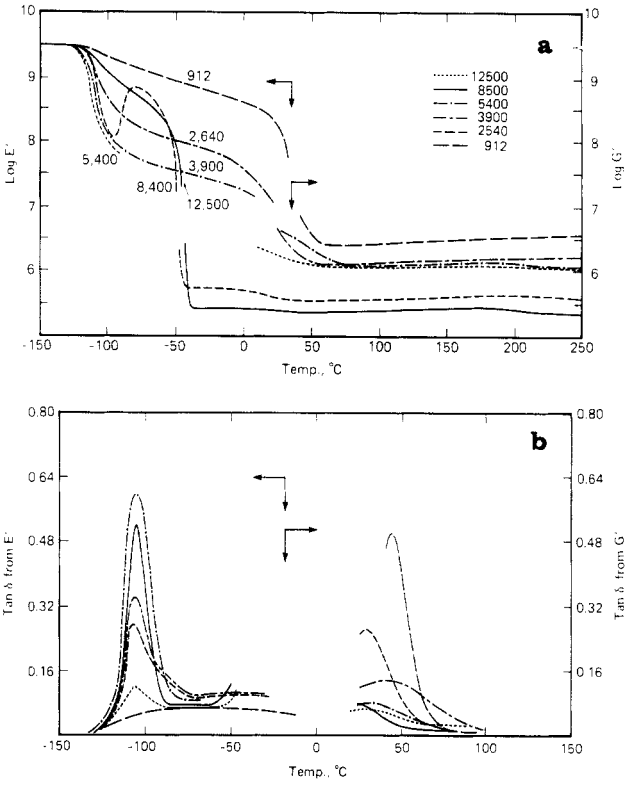


**Figure 3.** (a) Storage tensile and shear modulus versus temperature. (b) tan $\delta$ versus temperature for those networks synthesized via the monomer–oligomer approach.

blocks as reported in similar siloxane–urea segmented copolymers.[26] The $T_g$ of the hard segment is significantly depressed from that of high molecular weight homopoly(hydroxy ether) (100 °C). This can be attributed to the low molecular weight of the oligomer and a partial mixing of the phases.

A low $T_g$ was also observed in these network structures, characteristic of the soft-component poly(dimethylsiloxane). The $T_g$ values of the networks containing the lower siloxane block lengths were somewhat higher and broader than those of the oligomers. This suggests at least partial phase mixing in the soft segment phase. The networks containing the higher siloxane block lengths show sharp $T_g$ values that are identical with those of the oligomers (-120 °C). Those networks containing the 8500 and 12 400 g/mol siloxane segments show a clear melting endotherm due to the crystallization of the soft segment.

The dynamic mechanical behavior for the segmented copolymers prepared by the monomer–oligomer synthetic route is shown in Figure 3. The tensile modulus $E'$ was measured up to the $T_g$ of the hard block, and thereafter the shear modulus $G'$ was measured due to the rubbery nature of the sample. In all cases, the equation $E' = 3G'$ was found to be consistent with the data. Dynamic mechanical results clearly illustrate the two-phase morphology of the poly(hydroxy ether–siloxane) networks. The broad low-temperature transition in both the storage modulus and the tan $\delta$ for specimens containing the 900 g/mol PSX segment indicate a significant amount of mixing in the siloxane phase. As the molecular weight of the siloxane oligomer increases, the soft-segment $T_g$ shifts to lower temperatures (-120 °C) and becomes sharper. Accordingly, the rubbery modulus of the networks and the hard-segment $T_g$ decrease with increasing siloxane block length, complimenting the DSC results shown in Table III. The networks containing the 8400 and 12 400 g/mol siloxane oligomers show the crystallization and melting (~-40) of

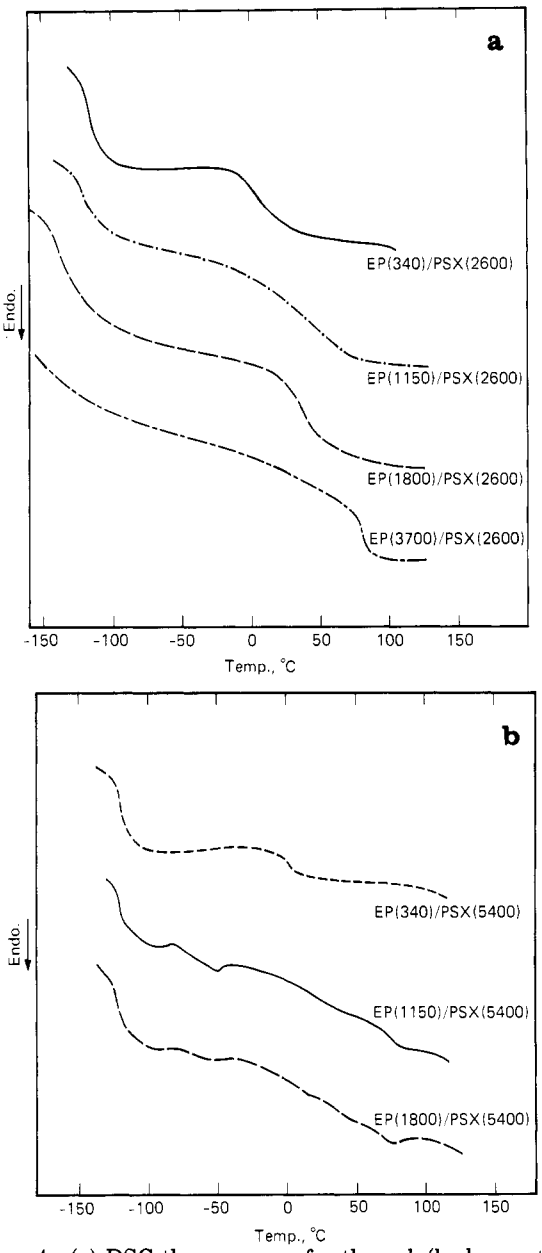


**Figure 4.** (a) DSC thermograms for the poly(hydroxy ether–siloxane) networks synthesized via the oligomer–oligomer route having a siloxane block length of 2600 g/mol and hydroxy ether block lengths varying from 340 to 3700 g/mol. (b) DSC traces for the poly(hydroxy ether–siloxane) networks synthesized via the oligomer–oligomer route having a siloxane block length of 5400 g/mol and hydroxy ether block lengths varying from 340 to 1800 g/mol.

the soft component. The modulus decreases sharply at the $T_g$ (−120 °C) and then increases with the crystallization of the siloxane and drops off again with the melting. Finally, the modulus above the $T_g$ of the hard segment increases with temperature, as would be predicted from rubber elasticity theory.[42,43]

In the second synthetic approach using the oligomer–oligomer route, aminopropyl-terminated poly(dimethylsiloxane) oligomers of block lengths 2600 and 5400 g/mol were chosen to react with the various molecular weight poly(hydroxy ether) oligomers (Scheme III). Table IV contains the molecular weight of the initial block lengths of each of the components, weight percent hard segment, and thermal transitions of the networks. As in the monomer–oligomer case, these materials displayed two $T_g$ values. Figure 4 shows DSC thermograms for the poly(hydroxy ether–siloxane) copolymers containing the 2600 and 5400 g/mol block lengths, respectively, which clearly illustrate the microphase separation of these polymers. Sample 2 in Table IV comprised of the 2600 g/mol siloxane block and the 1150 g/mol poly(hydroxy ether) block has a soft-segment $T_g$ (−116 °C) somewhat higher than that of the homopolysiloxane oligomer (−120 °C). However, networks containing higher hydroxy ether block lengths (1800 and 3700 g/mol) manifest a $T_g$ identical with that of the homopolysiloxane. Increasing the siloxane block length to 5400 g/mol results in markedly different behavior in that, regardless of the molecular weight of the hydroxy ether segment, a soft-segment $T_g$ of ca. −120 °C, comparable to that of the homopolysiloxane, is found. The molecular weight of both the hard and soft segments contribute to the extent of phase separation or, more precisely, the phase purity of the soft-segment phase.

Figure 5 contains the dynamic mechanical analysis of the networks containing the 2600 g/mol siloxane blocks. The tensile modulus was measured up to the $T_g$ of the hard segment, and the shear modulus was measured in the rubbery region. The low-temperature tan δ dampening peak and the storage modulus drop are clearly shifted to lower temperatures with increasing hydroxy ether block

**Table IV**
**Characteristics of Segmented or Block Poly(hydroxy ether–siloxane) Networks**

| | $M_n$, g/mol | | wt % hard | thermal analysis[a] of networks, °C | | | |
|---|---|---|---|---|---|---|---|
| no. | PSX | epoxy | segment | $T_g$[b] | $T_c$[b] | $T_m$[b] | $T_g$[c] |
| 1 | 2600 | 340 | 24 | −110 | | | 12 |
| 2 | 2600 | 1150 | 49 | −116 | | | 43 |
| 3 | 2600 | 1800 | 60 | −120 | | | 50 |
| 4 | 2600 | 3700 | 75 | −120 | | | 76 |
| 5 | 5400 | 340 | 13 | −120 | | | 10 |
| 6 | 5400 | 1150 | 31 | −120 | −70 | −50 | 75 |
| 7 | 5400 | 1800 | 41 | −120 | −70 | −50 | 75 |

[a] DSC, 10 °C/min heating rate. [b] Soft segment. [c] Hard segment.

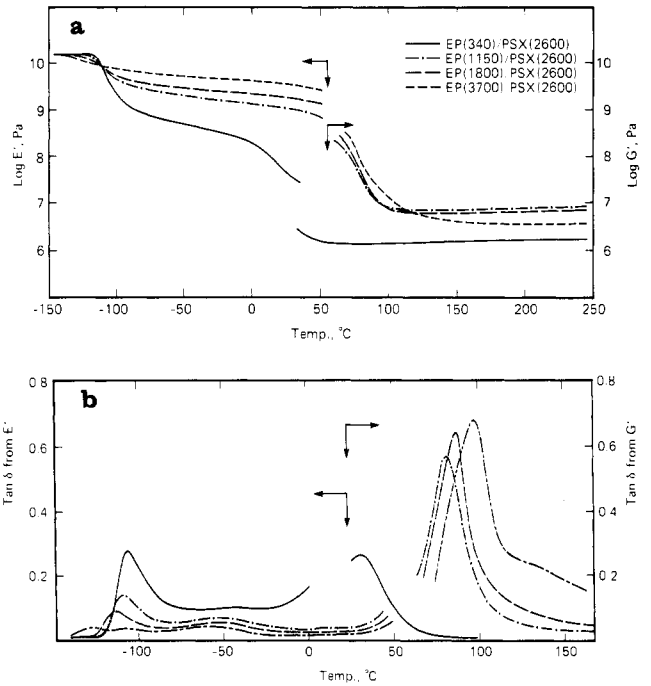


**Figure 5.** (a) Storage tensile and shear modulus versus temperature. (b) tan δ versus temperature for those networks, synthesized via the oligomer–oligomer route having a siloxane block length of 2600 g/mol and hydroxy ether block lengths varying from 340 to 3700 g/mol.

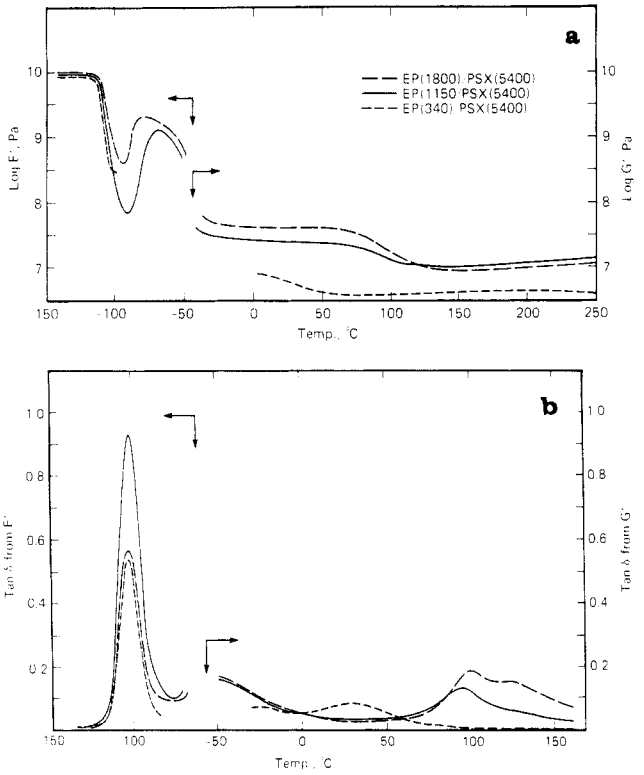


**Figure 6.** (a) Storage tensile and shear modulus versus temperature. (b) Tan $\delta$ versus temperature for those networks, synthesized via an oligomer–oligomer route having a siloxane block length of 5400 g/mol and hydroxy ether block lengths varying from 340 to 1800 g/mol.

lengths. Furthermore, the breadth of the transition decreases with higher hydroxy ether block lengths, suggesting a more well-defined siloxane or soft-segment phase.

The use of various molecular weight poly(hydroxy ether) block lengths with the 2600 g/mol siloxane oligomer produces a network structure with a higher $T_g$ (up to 76 °C) as shown in Figure 5 and in Table IV and improved dimensional stability. The $T_g$ of the hard-segment block of hydroxy ether component is somewhat depressed from that of the hydroxy ether oligomers except for the network containing the highest hydroxy ether block. Consequently, there is a strong dependence of the phase purity on the molecular weight of the hydroxy ether as well as the siloxane block.

The dynamic mechanical behavior for the copolymers containing the 5400 g/mol siloxane block are shown in Figure 6. These data, consistent with the DSC results, reflect the two-phase morphology. The tan $\delta$ damping peaks of the soft segment in the networks are identical with those of the siloxane oligomers (−120 °C), indicating minimal phase mixing in the siloxane component. Crystallization of the siloxane block may also be observed in the upturn in the storage modulus, $E'$, as well as the melting accompanied by a decrease in $E'$ at ~−40 °C. This is observed only for those samples containing the higher poly(hydroxy ether) blocks. As in the previous cases, the storage modulus between the $T_g$ of the siloxane and hydroxy ether segments is a function of the weight percent of the hard-segment component.

The thermal transitions of the hard segment for those networks containing the 5400 g/mol siloxane block exhibit a behavior that is very different from that of the networks previously described. The $T_g$ values are significantly higher than those for the poly(hydroxy ether) oligomers of comparable molecular weight (Table IV). There are several competing factors involved, including phase mixing,

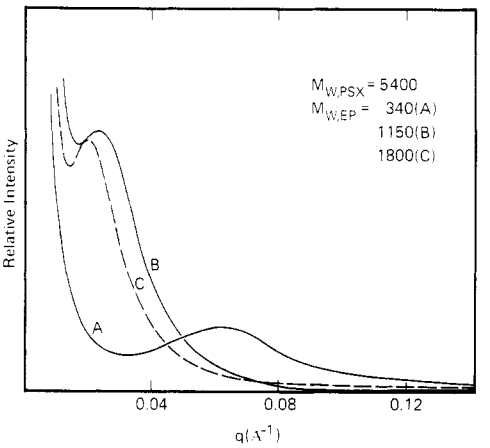


**Figure 7.** Small-angle X-ray scattering profiles for a series of poly(hydroxy ether–siloxane) networks where the molecular weight of the siloxane segment is fixed at 5400 g/mol and the molecular weight of the epoxy block is varied as indicated.

which tends to decrease the $T_g$, and chain-end cross-linking, which tend to increase the $T_g$. The purity of the siloxane phase is sufficient to allow crystallization of the siloxane block. Thus, it appears as if cross-linking of the chain ends confines the chain segments sufficiently to increase $T_g$.

Typical small-angle X-ray scattering (SAXS) profiles for the poly(hydroxy ether–siloxane) copolymers are shown in Figure 7 as a function of the scattering vector $q$ with a magnitude given by $4\pi/\lambda \sin \epsilon/2$, where $\lambda$ is the wavelength and $\epsilon$ is the scattering angle. In all cases, the scattering curves exhibit a single diffuse maximum whose position depends upon the molecular weights of the hard- and soft-segment molecular weights. The scattering profile of the EP(340)/PSX(5400) shown in Figure 7 typifies that observed for the monomer–oligomer preparation discussed previously. Here, the SAXS reflection is quite diffuse, with a maximum occurring near 70 Å regardless of the molecular weight of the siloxane segment. As a measure of the breadth of the distribution of the phase sizes giving rise to the scattering, the full width at half-maximum relative to the peak position can be used. For these monomer–oligomer networks values of $\Delta q/q_{max} \simeq 0.7$ are found. Analysis of the high scattering vector portion of the SAXS profiles, using a Porod analysis, yields a transition-zone thickness or the diffuse-phase boundary between the phases that is very narrow (ca. 10 Å).

The networks prepared via the oligomer–oligomer approach exhibit different characteristics. Here, the long period corresponding to the position of the peak maximum ranges from 70 to 250 Å, depending on the molecular weight of the hard segments, and the values of $\Delta q/q_{max}$ are found to be 1.31, nearly 60% larger that observed for the monomer–oligomer preparation. In addition, the diffuse-phase boundary is on the order of 35 Å, significantly broader that of the monomer–oligomer preparation.

These differences can be directly related to the molecular weight distributions of the hard- and soft-segment phases. For the monomer–oligomer approach the thickness distribution function of the hard segment phase is basically a $\delta$ function corresponding to the length of the epoxy monomer. It is evident from the thermal and mechanical properties presented previously that the monomer sequences form a distinct phase. Swelling studies to be discussed later suggest strongly that hydrogen bonding between the hard segments provides the driving force to align these monomer sequences, thereby producing the relatively sharp phase boundaries observed. For the oli-

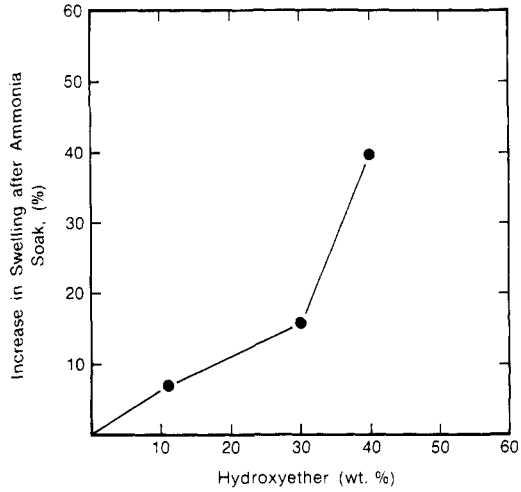


**Figure 8.** Percent increase in swelling after ammonia soak versus weight percent hard block.

gomer–oligomer networks, however, the sequence length distribution for the hard-segment phase is broad ($M_W/M_n$ = 2.0–2.5). Provided these sequences align in a manner similar to that in the monomer–oligomer preparation, the sequence length distribution of the hard segments will give rise to a diffuse interface, as is observed experimentally.

It is important to address the forces that cause the formation of the microphase-separated morphology in the monomer–oligomer networks. Results of calorimetric, dynamic mechanical, and scattering measurements clearly indicate microphase separation. This result is somewhat surprising since isolated epoxy segments, together with the end groups of the siloxane oligomer, form the hard-segment phases. Even though the solubility parameters of the soft and hard segments are considerably different, 7.3 and 9.6, respectively, it is unlikely that this is the sole driving force for the microphase separation, since the molecular weight of each segment is low and they are incorporated into a copolymer. It is far more likely that hydrogen bonding between the segments represents the dominant force. Quantitative evaluation of the extent of hydrogen bonding is difficult, but swelling measurements prior to and after exposure to ammonia provide a means of detecting the presence of hydrogen bonding. Thus, a series of the networks was swollen with chloroform where the molecular weight of the siloxane segment was fixed at 5400 g/mol, and the hard-segment molecular weight was varied. The weight uptake was measured after a 72-h period. The networks were then exposed to ammonium and chloroform vapors, and the weight uptake was measured after another 72 h. The ammonium vapors tend to disrupt hydrogen bonding and thus should give rise to an enhanced solvent uptake. In Figure 8 is shown the percent increase in swelling as a function of the weight percent of hard block. A dramatic increase in the swelling was found for all the hard-segment molecular weights studied. In fact, the swelling increase is directly proportional to the amount of hard segment. Thus, the extent of hydrogen bonding in the hard-segment phase must be extensive, which must contribute substantially to the observed phase separation.

The position of the SAXS long period reflecting the average center-to-center distance of adjacent hard- or soft-segment phases was found to depend upon the molecular weight of the two phases. In Figure 9, the Bragg spacing, $d$, corresponding to the maximum of the scattering profile is shown as a function of the soft-segment molecular weight for the monomer–oligomer network preparation. The separation distances between the hard-segment phases

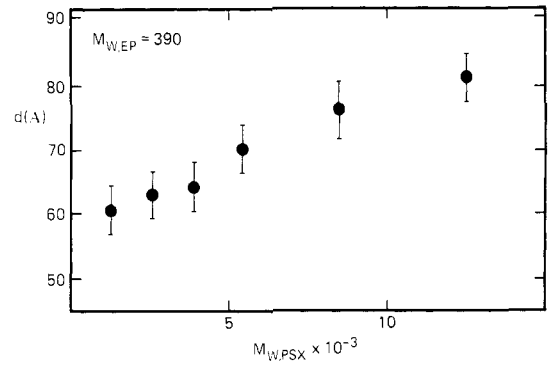


**Figure 9.** Dependence of the SAXS long period as a function of the molecular weight of the epoxy segment for the poly(hydroxy ether–siloxane) networks prepared via the monomer–oligomer synthesis.

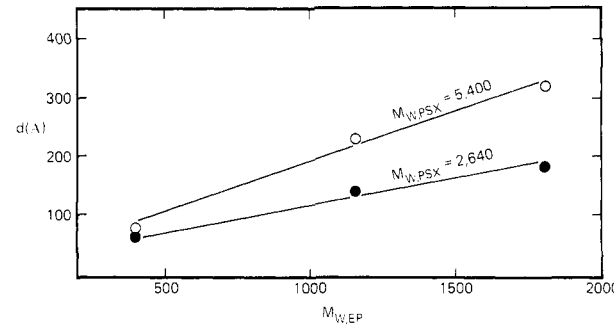


**Figure 10.** Bragg spacing corresponding to the position of the maximum in the scattering profiles as a function of the molecular weight of the hard segment for poly(hydroxy ether–siloxane) networks where the molecular weights of the siloxane segments are 2640 and 5400 g/mol.

are found to depend only weakly on the siloxane molecular weight. Such a weak dependence of the separation distance is quite surprising. In contrast to these data, the dependence of the long period on the molecular weight of the hydroxy ether segment was found to be much stronger for two networks where $M_{PSX}$ = 2640 and 5400 g/mol as shown in Figure 10. If it is assumed that $d \propto M^x$, for the monomer–oligomer preparation, $x$ is found to be 0.13, whereas for the oligomer–oligomer preparation, $x$ is 0.83 and 0.62 for the 2640 and 5400 g/mol polysiloxane molecular weights, respectively. Due to the low molecular weights of both the hard and soft segments, the distribution of the segment lengths, and the multiblock nature of the copolymers, it is not possible to draw quantitative conclusions from these exponents. However, the dramatic difference between the effects of the soft- and hard-segment lengths is noteworthy.

The retention of the mechanical properties at elevated temperatures in these systems requires that the hard- and soft-segment phases remain microphase separated. In Figure 11, the dependence of the SAXS on temperature is shown from 30 to 240 °C at a scanning rate of 10 °C/min. The intensity of the SAXS was found to increase by nearly 40% over this temperature interval, whereas the long period increased by only 4%. The dependence of the total integrated scattering or the scattering invariant $Q$ on temperature is shown in Figure 12. Here the dramatic increase in the scattering is clearly evident. These results, however, do not suggest that the phases are becoming more pure at elevated temperatures. In fact, the invariant of the room-temperature profile is $4.95 \times 10^{-3}$ (mol $e^-/cm^3)^2$, which compares to a calculated value of $4.68 \times 10^{-3}$ (mol $e^-/cm^3)^2$ assuming that the hard- and soft-segment phases are pure. This close agreement suggests that the major

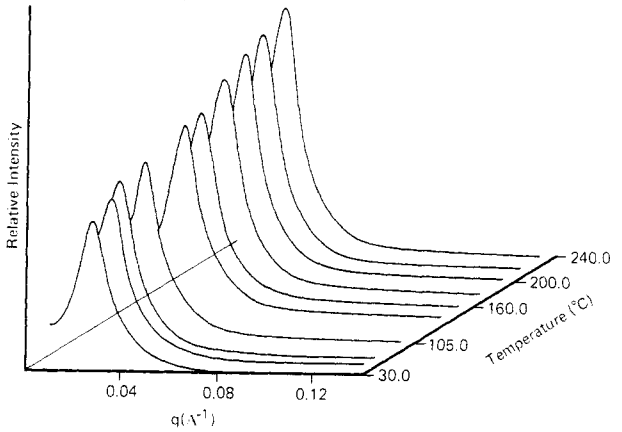


**Figure 11.** Intensity as a function of scattering vector for a poly(hydroxy ether–siloxane) network collected over a temperature interval ranging from 40 to 240 °C at a scanning rate of 10 °C/min. The scattering profiles are for a sample where $M_{PSX}$ = 5,400 and $M_{EP}$ = 1,150 g/mol.

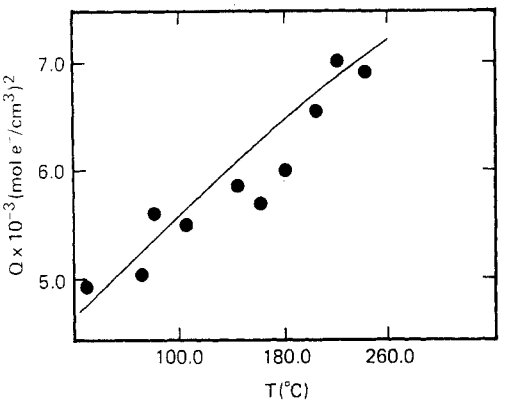


**Figure 12.** Invariants or integrated scattering as a function of temperature obtained from the scattering profiles shown in Figure 11. The line drawn represents values calculated by using the thermal expansion coefficients of the two phases and eq 4.

changes result from sources other than enhanced purity at elevated temperatures. The key to the dramatic increase in the total scattering and the small charge in the long period lies with the coefficient of thermal expansion.

For the data shown in Figure 11 the long period at 20 °C is 232 Å. With use of tabulated values of the linear thermal expansion coefficients[44] for the epoxy and siloxane phases, a long period of 245 Å would be expected at 240 °C. This 5.6% increase in the long period is in good agreement with the experimental observations. The total integrated scattering is given by

$$Q = \phi_S\phi_H(\rho_S - \rho_H)^2 \quad (1)$$

where $\phi_S$ and $\phi_H$ are the volume fractions of the soft- and hard-segment phases with electron densities of $\rho_S$ and $\rho_H$, respectively. For determination of the temperature dependence of the invariant, eq 1 is differentiated with respect to temperature yielding

$$dQ/dT = \phi_S\phi_H(\alpha_S - \alpha_H)(\phi_H - \phi_S)(\rho_S - \rho_H)^2 + 2\phi_S\phi_H(\rho_S - \rho_H)(\rho_H\alpha_H - \rho_S\alpha_S) \quad (2)$$

where $\alpha_S$ and $\alpha_H$ are the volume thermal expansion coefficients of the soft- and hard-segment phases. The volume expansion coefficient is simply 3 times the linear expansion coefficient of the phases. Equation 2 can be rewritten as

$$\frac{dQ}{dT} = Q\left\{(\phi_H - \phi_S)(\alpha_S - \alpha_H) + 2\frac{\rho_H\alpha_H - \rho_S\alpha_S}{\rho_s - \rho_H}\right\} \quad (3)$$

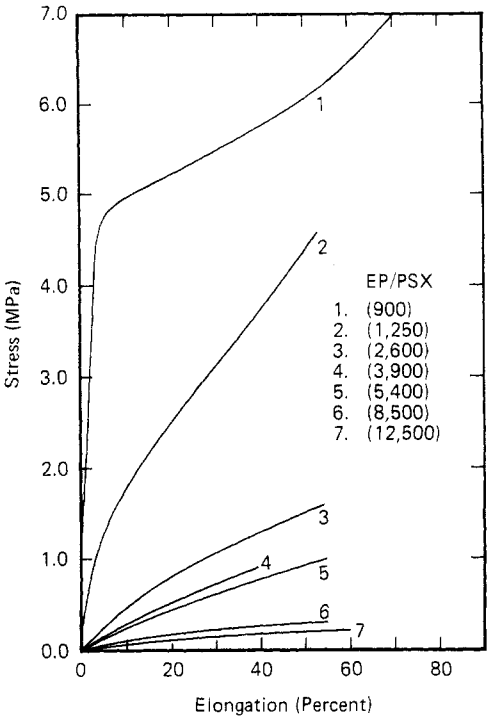


**Figure 13.** Stress versus percent elongation for the networks prepared via the monomer–oligomer synthetic approach having siloxane block length varying from 900 to 12 400 g/mol.

**Table V**
**Mechanical Properties of Poly(hydroxy ether–siloxane) Networks**

| sample | modulus, MPa | tensile strength, MPa | elongation to break, % |
|---|---|---|---|
| PDMS network | 0.5 | 0.4 | 70 |
| Ep\|PSX(912) | 153.0 | 7.0 | 70 |
| Ep\|PSX(1250) | 40.0 | 4.6 | 53 |
| Ep\|PSX(2650) | 4.5 | 1.6 | 55 |
| Ep\|PSX(3300) | 3.0 | 0.9 | 40 |
| Ep\|PSX(5400) | 2.5 | 1.0 | 55 |
| Ep\|PSX(8500) | 1.0 | 0.4 | 55 |
| Ep\|PSX(12,400) | 0.6 | 0.3 | 60 |

Therefore, the change in the invariant from a temperature $T_1$, $Q_{T_1}$, to a temperature $T_2$, $Q_{T_2}$, is given by

$$Q_{T_2} = Q_{T_1}\left\{1 + \left[(\phi_H - \phi_S) \times (\alpha_S - \alpha_H) - 2\frac{\rho_S\alpha_S - \rho_H\alpha_H}{\rho_S - \rho_H}\right](T_2 - T_1)\right\} \quad (4)$$

Using tabulated values of the linear thermal expansion coefficients the increase in the invariant from $4.95 \times 10^{-3}$ to 0 $7.3 \times 10^{-3}$ (mol e$^-$/cm$^3$)$^2$ when the temperature is raised from 25 to 26 °C is easily accounted for. In Figure 12 the calculated invariant is compared with the experimentally observed values. As can be seen, the agreement is quite reasonable over the entire temperature range studied.

**Mechanical Properties and Toughening Mechanisms.** The mechanical properties of poly(hydroxy ether–siloxane) copolymers range from a rubber-toughened thermoplastic to a thermoplastic elastomer depending on the relative composition of the copolymer. The stress versus percent elongation for the poly(hydroxy ether–siloxane) networks synthesized by the monomer–oligomer route is shown in Figure 13. These data are also included in Table V. The ultimate elongations range from 40 to

**Table VI**
**Mechanical Properties of Poly(hydroxy ether–siloxane) Networks**

| sample | modulus, MPa | yield stress, MPa | yield strain, % | tensile strength, MPa | elongation to break, % |
|---|---|---|---|---|---|
| PDMS network | 0.5 | | | 0.4 | 70 |
| EP340\|PSX(2640) | 4.5 | | | 1.6 | 55 |
| EP340\|PSX(5400) | 2.5 | | | 1.0 | 46 |
| EP1150\|PSX(2640) | 155.0 | | | 12.0 | 180 |
| EP1150\|PSX(5400) | 3.0 | | | 1.4 | 63 |
| EP1800\|PSX(2640) | 330.0 | 15 | 7.5 | 19.0 | 175 |
| EP1800\|PSX(5400) | 3.5 | | | 1.5 | 55 |
| EP3700\|PSX(2640) | 600.0 | 32 | 10.0 | 29.0 | 80 |

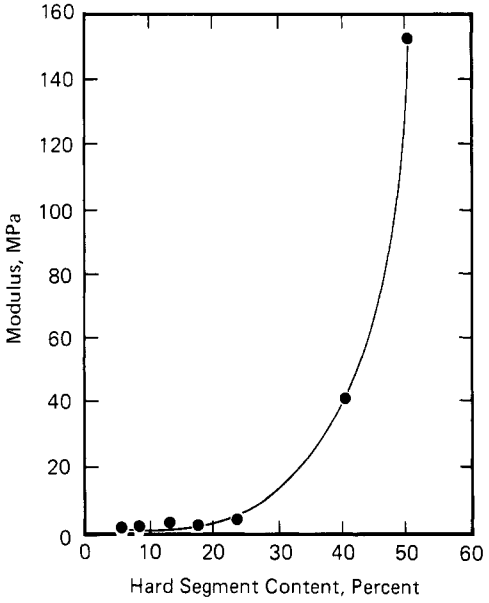


**Figure 14.** Modulus versus weight percent hard segment for those networks prepared via the monomer–oligomer approach.

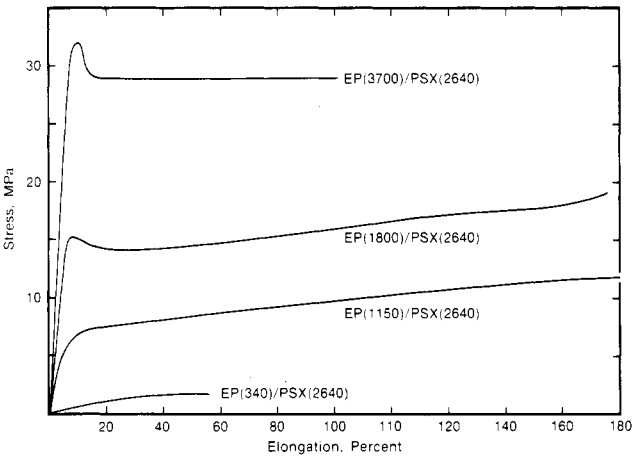


**Figure 15.** Stress versus percent elongation for the poly(hydroxy ether–siloxane) copolymers having a siloxane block length of 2600 g/mol and hydroxy ether block length varying from 340 to 3700 g/mol.

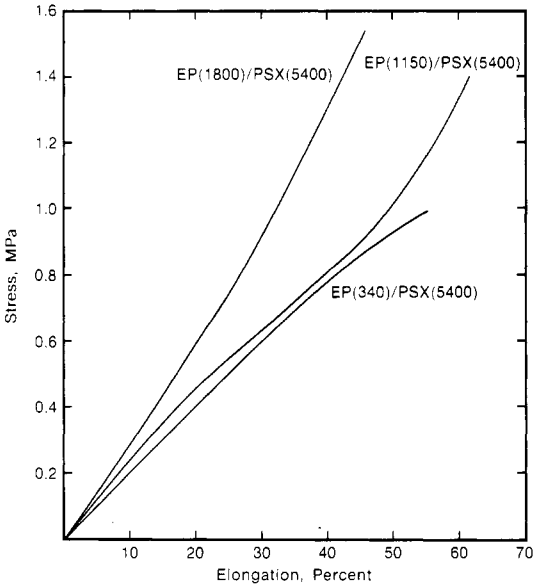


**Figure 16.** Stress versus percent elongation for the poly(hydroxy ether–siloxane) copolymers having a siloxane block length of 5400 g/mol and hydroxy ether block length varying from 340 to 1800 g/mol.

60%, and the moduli vary from 0.5 to 150.0 MPa depending on the molecular weight of the siloxane oligomer used. The networks containing the higher hard-segment contents show a higher modulus, and the sample containing 50 wt % hard segment shows mechanical behavior approaching that of ductile yielding. This suggests at least partial continuity in the hard-segment phase. For further illustration of this point, Figure 14 shows the modulus as a function of the weight percent hard segment. The sharp drop in modulus with increasing hard-segment content clearly reflects phase inversion where the siloxane phase becomes continuous. However, it is important to bear in mind that the $T_g$ of the networks containing the lower siloxane block lengths have a slightly higher hard-segment $T_g$, which may affect the mechanical behavior.

The stress versus elongation plots for the segmented poly(hydroxy ether–siloxane) networks containing the chain-extended hydroxy ether block synthesized by the oligomer–oligomer route are shown in Figures 15 and 16. These data are summarized in Table VI. Here, the soft-segment molecular weight was either 2600 or 5400 g/mol, and the hard-segment molecular weight varied from 340 to 3700 g/mol. The networks containing the 5400 g/mol siloxane block showed only marginal improvements in mechanical properties with longer hydroxy ether block lengths. This is not surprising since the siloxane phase is continuous in all cases. In contrast, the networks containing the 2600 g/mol siloxane oligomer showed markedly different behavior. In this case, the morphology of copolymers contributes significantly to the mechanical properties, particularly when the hydroxy ether is the continuous phase. The moduli increase from 4.5 to 600 MPa and the tensile strength increases depending on the block lengths. Samples EP(3700)/PSX(2600) and EP(1800)/PSX(2600) where the hydroxy ether forms a continuous phase show ductile yielding and necking, indicating permanent or plastic deformation in the continuous hard phase.

Tables V and VI also contain the modulus and ultimate properties of a poly(dimethylsiloxane) (PDMS) network which is used as a comparison to the poly(hydroxy ether–siloxane) networks where the siloxane component is the

**Table VII**
**Predicted Modulus Values versus Experimental Data for the Copolymers According to Kerner's Analysis**

| sample | vol fraction hard segment, $\theta_{Ep}$ | predicted morphology | modulus, MPa | |
|---|---|---|---|---|
| | | | theor | exptl |
| Ep(340)\|PSX(5400) | 0.11 | spherical | 2.5 | 2.5 |
| Ep(1150)\|PSX(5400) | 0.29 | cylindrical | 4.0 | 3.0 |
| Ep(1800)\|PSX(5400) | 0.39 | cylindrical | 5.0 | 3.5 |
| Ep(340)\|PSX(2600) | 0.20 | spherical | 3.2 | 4.5 |
| Ep(1150)\|PSX(2600) | 0.46 | lamellar | | |
| Ep(11800)\|PSX(2600) | 0.57 | lamellar | 1400.0 | 330.0 |
| Ep(3700)\|PSX(2600) | 0.73 | cylindrical | 1500.0 | 600.0 |

continuous phase. Clearly, the heterogeneous morphology has a large influence on the mechanical properties. Interfacial adhesion occurs between the dispersed hydroxy ether phase and the siloxane phase through chemical bonding of the two dissimilar components. The incorporation of the dispersed hydroxy ether phase serves to increase the internal of the PDMS network in a manner similar to the hard domains in segmented polyurethanes[12,13] and filled siloxan elastomers.[51] This retards chain mobility, thereby reducing the initiation and propagation of microcracks. In some instances, the $T_g$ of the hydroxy ether phase is near ambient temperatures, and in these cases reinforcement is achieved but to a lesser extent than when the hydroxy ether $T_g$ is high.

Generally, in a two-phase system, the continuous phase dominates the mechanical properties. For the case of a discrete phase embedded in a matrix of the second component, the mechanical properties may be predicted by using Kerner's analysis,[45] which is often used to predict the modulus of block copolymers and block copolymer/homopolymer blends. The modulus of the composite is given by

$$E = E_c\left[\frac{V_dE_d}{(7-5\nu_c)E_c+(8-10\nu_c)E_d}+\frac{V_c}{15(1-\nu_c)}\right]\Bigg/\left[\frac{V_dE_c}{(7-5\nu_c)E_c+(8-10\nu_c)E_d}+\frac{V_c}{15(1-\nu_c)}\right] \quad (5)$$

where $E_d$ and $E_c$ are the moduli of the dispersed and discrete phases, with Poisson's ratios $\nu_d$ and $\nu_c$ and volume fractions $V_d$ and $C_c$, respectively.

Two series of network structures were examined where the soft block was held constant at 2600 and 5400 g/mol and the hard-segment block length was varied. Table VII contains the volume fraction, theoretically predicted morphology and modulus, and the experimentally measured modulus for the various copolymers. For those samples where spherical morphology is predicted, reasonably good agreement is seen between the measured modulus and that predicted. However, at higher volume fractions of hard segment, the agreement between theory and experiment gets progressively worse. This clearly reflects a morphology transition from spherical to either cylindrical or lamellae of the epoxy phase, which invalidates the assumptions implicit in eq 2. This is consistent with other siloxane-containing block copolymer systems previously reported.[22]

## Summary

Segmented or block poly(hydroxy ether–siloxane) copolymers were synthesized by both monomer–oligomer and oligomer–oligomer synthetic approaches. Perfectly alternating sequence distributions were obtained from the monomer or oligomer(s) bearing mutually reactive end groups, and the hydrox ether linkage is formed simultaneously with the growth of the second block. DSC, DMTA, and SAXS results demonstrated that microphase-separated morphologies were achieved for each of the copolymers, even those structures synthesized by the monomer–oligomer route. The mechanical properties of the networks depended upon the morphology and ranged from a rubber-toughened thermoplastic to a thermoplastic elastomer.

**Registry No.** (DGEBA)($D_4$) (block copolymer), 114533-79-8; (Epon 1001F)($D_4$) (block copolymer), 114533-80-1.

## References and Notes

(1) Smith, T. L. In *Rheology*, 5th ed.; Eirch, F. R., Ed.; Academic: New York, 1969.
(2) Warrick, E. L.; Pierce, O. R.; Polmanteer, K. E.; Saam, J. C. *Rubber* Chem. *Technol.* **1979**, *52*, 437.
(3) Mark, J. E.; Kato, M. *J. Polym. Sci. Polym. Symp.* **1976**, *54*, 217.
(4) Andrady, A. L.; Llorente, M. A.; Mark, J. E. *J. Chem. Phys.* **1980**, *72*, 2282.
(5) Tang, M. Y.; Mark, J. E. *Macromolecules* **1984**, *17*, 2616.
(6) Mark, J. E. *Adv. Polym. Sci.* **1982**, *44*, 1.
(7) Mark, J. E. *Elastomers and Rubber Elasticity*; Mark, J. E., Lai, J., Eds.; American Chemical Society: Washington, DC, 1982.
(8) Haidar, B.; Smith, T. L. *Polym. Mater. Sci. Eng.* **1986**, *55*, 164.
(9) Noshay, A.; McGrath, J. E. *Block Copolymers, Overview and Critical Survey*; Academic: New York, 1977.
(10) Smith, T. L. *Rubber Chem. Technol.* **1978**, *51*, 225.
(11) *Block Copolymers*; Allport, D. C., James, W. H., Eds.; Wiley: New York, 1973.
(12) Smith. T. L. *J. Polym. Sci., Polym. Phys. Ed.* **1974**, *12*, 1825.
(13) Smith, T. L. *Polym. Eng. Sci.* **1977**, *17*, 129.
(14) Smith, T. L. *Elastomers and Rubber Elasticity*; Mark, J. E., Lai, J., Eds.; American Chemical Society: Washington, DC, 1982.
(15) Noshay, A.; Matzner, M.; Merriam, C. N. *J. Polym. Sci., Polym. Chem. Ed.* **1971**, *9*, 3147.
(16) Tyagi, D.; Hedrick, J. L.; Webster, D. C.; McGrath, J. E.; Wilkes, G. L. *J. Appl. Polym. Sci.*, in press.
(17) Matzner, M.; Noshay, A.; Robeson, L. M.; Merriam, C. N.; Barclay, R.; McGrath, J. E. *Appl. Polym. Symp.* **1973**, *22*, 143.
(18) Brandt, P. J. A.; Webster, D. C.; McGrath, J. E. *Polym. Prepr. (Am. Chem. Soc., Div. Polym. Prepr.)* **1984**, *25* (2), 91.
(19) Riffle, J. S.; Freelin, R. G.; Banthia, A. K.; McGrath, J. E. *J. Macromol. Sci., Chem.* **1981**, *A15*, 967.
(20) Riffle, J. S. Ph.D. Thesis, Virginia Polytechnic Institute and State University, 1981.
(21) LeGrand, D. G. *J. Polym. Sci., Part B* **1969**, *7*, 579.
(22) Robeson, L. M.; Noshay, A.; Matzner, M.; Merriam, C. N. *Angew. Makromol. Chem.* **1973**, *47*, 29130.
(23) Yilgor, I.; et al. *Polym. Prepr. (Am. Chem. Soc., Div. Polym. Chem.)* **1983**, *24* (1), 167.
(24) Tran, C. Ph.D. Thesis, Virginia Polytechnic Institute and State University, 1985.
(25) Yilgor, I.; Riffle, J. S.; Wilkes, G. L.; McGrath, J. E. *Polym. Bull.* **1982**, *8*, 535.
(26) Tyagi, D.; Wilkes, G. L.; Yilgor, I.; McGrath, J. E. *Polym. Bull.* **1982**, *8*, 543.
(27) Hedrick, J. L.; Haidar, B.; Hofer, D. C.; Tran, C.; McGrath, J. E. *Polym. Prep. (Am. Chem. Soc., Div. Polym. Chem.)* **1986**, *27* (2), 203.
(28) Hedrick, J. L.; Haidar, B.; Russell, T. P.; Hofer, D. C. *Polymer Prepr. (Am. Chem. Soc., Div. Polym. Chem.)* **1987**, *28* (1), 99.
(29) Vonk, G. C. *J. Appl. Crystallogr.* **1971**, *47*, 340.
(30) Glatter, O. *Acta Phys. Austriaca* **1977**, *47*, 83.
(31) Glatter, O. *J. Appl. Crystallogr.* **1977**, *10*, 415.
(32) Stephenson, G. B. Thesis, Stanford University, 1982.
(33) Russell, T. P.; Koberstein, J. T. *J. Polym. Sci., Polym. Phys. Ed.* **1985**, *23*, 1109.
(34) Riffle, J. S.; Yilgor, I.; Tran, C.; Wiles, G. L.; McGrath, J. E. *Epoxy Resin-II*; Bauer, R. S., Ed.; ACS Symposium Series 221; American Chemical Society: Washington, DC, 1983; Chapter 2.
(35) Kantor, S. W.; Grubb, W. T.; Osthoff, R. C. *J. Am. Chem. Soc.* **1954**, *76*, 5190.

(36) Wnuk, A. J.; Davidson, T. F.; McGrath, J. E. *J. Appl. Polym. Sci., Appl. Polym. Symp.* **1978**, *34*, 89.
(37) Reinking, N. H.; Barnebeo, A. E.; Hale, W. F. *J. Appl. Polym. Sci.* **1963**, *7*, 2135.
(38) Hale, W. F. *Encyclopedia of Polymer Science and Technology*; **1969**, *10*, 111.
(39) Reinking, N. H.; Barnabeo, A. E.; Hale, H. F. *J. Appl. Polym. Sci.* **1963**, *7*, 2145.
(40) Myers, G. E.; Dagon, J. R. *J. Polym. Sci., Polym. Chem. Ed.* **1964**, *2*, 2631.
(41) Senger, J. S.; Subramanian, R.; Ward, T. C.; McGrath, J. E. *Polym. Prep. (Am. Chem. Soc., Div. Polym. Chem.)* **1986**, *27* (2), 144.
(42) Flory, P. J. *Principles of Polymer Chemistry*; Cornell University Press: Ithaca, NY, 1953.
(43) Treloar, L. R. G. *The Physics of Rubber Elasticity*, 3rd ed.; Clarendon: Oxford, 1975.
(44) Van Krevelen, D. W. *Properties of Polymers*; Elsevier Scientific: Amsterdam, Netherlands, 1972.
(45) Kerner, E. H. *Proc. Phys. Soc., London Sect. B* **1956**, *69B*, 808.

# Polymerization of *N,N*-Didodecyl-*N*-methyl-*N*-(2-(methacryloyloxy)ethyl)ammonium Chloride, an Inverse Micelle Forming Detergent

**G. Voortmans, A. Verbeeck, C. Jackers, and F. C. De Schryver***

*The Department of Chemistry, K. U. Leuven Celestijnenlaan, 200F B-3030 Heverlee, Belgium.* *Received April 13, 1987*

ABSTRACT: In this paper the first results obtained on the polymerization of *N,N*-didodecyl-*N*-methyl-*N*-(2-(methacryloyloxy)ethyl)ammonium chloride, an inverse micelle forming detergent, are presented. A full characterization of the monomeric reverse micellar system is presented, from use of the fluorescence probe technique. The critical micelle concentration (cmc) of the monomer was determined to be $10^{-4}$ M. Fluorescence quenching and viscosity measurements were used to determined the aggregation number and dynamic character of the monomeric aggregates. The same experiments were carried out for the polymeric aggregates, and the results are compared with those of the monomeric aggregates. This comparison shows that the polymeric aggregates form inverse micellar systems. It is further proved that the dynamic character of the reverse micellar system is lowered upon polymerization. Gel permeation chromatography (GPC) analysis indicates that the polymerization of the monomer leads to high molecular weight polymers with a degree of polymerization several times larger than the aggregation number of the initial reverse micellar system.

## Introduction

The polymerization of monomers in the presence of detergents is well established in both aqueous and nonaqueous media.[1] Recently a strong interest has developed in the polymerization of some surfactant aggregates.[2-9] This is undoubtedly caused by the potential use of these systems, which could be further enhanced when stabilized by polymerization. Polymerization could combine the beneficial properties of stable polymer particles with the specific properties of micelles, microemulsions, and vesicles.[4] Considerable work has been done in the field of polymerization of vesicles, monolayers, and multilayers.[2-7] In contrast only a few reports exists on the polymerization of aqueous micellar systems.[8,9] The polymerization of a reverse micellar system has not yet been reported. This paper presents the first results obtained on the polymerization of a reverse micellar system of *N,N*-didodecyl-*N*-methyl-*N*-(2-(methacryloyloxy)ethyl)ammonium chloride (I) in toluene.

## Characteristics of the Monomer I

To determine in which cases the monomer can form reverse micellar structures, we tested a series of apolar solvents to evaluate the solubility of the monomer. In addition the amount of water soluble in these systems has also been investigated. If the monomer is soluble in the apolar solvent and can also solubilize water, one can then conclude that reverse micellar structures are formed.[10a] The results are presented in Table I. As benzene and toluene are solvents in which the monomer is soluble and in which it can also solubilize water, one can conclude that in these solvents the monomer forms reverse micellar structures.

**Table I**
**Monomer Solubility and Water Solubility in Various Solvents**

| solvent | monomer solubility | $R^a$ |
|---|---|---|
| benzene | *b* | 0 → 4 |
| toluene | *b* | 0 → 4 |
| cyclohexane | *c* | 0 → 2 |
| hexane | *d* | |

[a] $R = [H_2O]/[\text{monomer}]$. [b] Very soluble. [c] Soluble. [d] Insoluble.

An important characteristic of the monomer is its cmc. The meaning of this term in a reverse micellar system is somewhat different from that of aqueous micellar system.[10b] Eicke et al. proposed that in apolar media the surfactant AOT upon aggregation first forms linear aggregates, which then undergo a transformation to cyclic ones.[11] This last phenomenon is then called the cmc. It was found that the model of Eicke was also valid for ammonium surfactants.[10a] The cmc can be determined by monitoring the absorbance and/or fluorescence of a probe as a function of the logarithm of the surfactant concentration. From these properties, presented in Figures 1 and 2, it can be seen that there is aggregation of the monomer that leads to an increase in the absorbance of the probe (Figure 1). As the probe is already fully solubilized by the small linear aggregates, there is no second inflection in absorbance that would be caused by cyclization, so that one cannot determine the cmc from absorbance measurements. The cmc can however be determined by monitoring the fluorescence decay of the same probe as a function of the logarithm of the surfactant concentration. In Figure 2 the contribution of the long decay time of the probe is plotted as a function of the logarithm of the

0024-9297/88/2221-1977$01.50/0 